

## **Acknowledgements**

This work was supported by grants from Scientific Research from the Ministry of Health, Labor, and Welfare of Japan (WA2F2547) and from the Japan Society for the Promotion of Science (JSPS No. 2567046405) to M.N. and from the Hokuto Foundation for Bioscience to H.W.

We thank S. Takagi, K. Ikeda, M. Sato, M. Narasaki, and H. Nakamura for their technical assistance.

Human plasma samples were kindly provided by the Japanese Red Cross Society.

## **Author contributions**

H.W., S.M., H.T., and M.N. planned the study. H.W., S.M., Y.M., and M.S. performed the experiments using purified human neutrophils. Y.G. performed the experiments using vascular endothelial cells. H.W., K.L., H.T., and K.T. performed the sepsis mice experiments. A.O. and T.Y. analyzed neutrophil shape and histological features, respectively. K.K. and H.M. determined the plasma HRG in septic patients. H.W., S.M., and M.N. wrote the manuscript.

## **Additional information**

**Competing financial interests:** The authors declare no competing financial interests.

## Figure legends

Figure 1. HRG's effects on the mortality of CLP mice and the passage of neutrophils through microcapillaries.

(A) CLP was performed in mice, and plasma levels of HRG were determined 24 h after CLP by Western blotting. Quantification of the results of Western blotting. \*\*\*

P<0.001 vs. sham. (B) Kaplan-Meier survival curve of mice with CLP. PBS, HSA (20 mg/kg), or human purified HRG (4 or 20 mg/kg) was administered i.v. 10 min, 24 h, and 48 h after CLP. (C) Effects of knockdown of liver HRG by siRNA on the plasma

levels of HRG. The plasma levels were determined immediately before CLP by Western blotting. Quantification of the results of Western blotting. \*\*\* P<0.001 vs.

Control RNAi. (D) Effects of knockdown of liver HRG by siRNA on the survival of mild-CLP mice. (E) Determination of HRG mRNAs in the liver of CLP or

LPS-injected mice. The tissue samples for real-time PCR were collected 6 or 24 h after CLP or LPS injection. The relative expression levels of HRG mRNA in the liver were calculated as % of sham control. \*\*\*P< 0.001 vs. sham. (F) Plasma levels of

HRG were determined 6 or 24 h after CLP or LPS injection by Western blotting. The relative expression levels were calculated as % of sham control. \*P< 0.05, \*\*P< 0.01

and \*\*\*P< 0.001 vs. sham. (G) Decreased plasma HRG levels in human sepsis.

HRG levels were determined by ELISA. Individual symbols represent individual donors and horizontal lines indicate mean. \*\*\*P < 0.001 vs. normal. (H) *In vivo* imaging of circulating neutrophils in CLP mice. The neutrophils were labeled by i.v. injection of anti-Gr-1 antibody 24 h after CLP, and the circulating neutrophils were observed under an *in vivo* imaging system. Red arrowheads indicate the neutrophils attached to the vascular wall. Yellow arrowhead indicates the neutrophil involved in stopping the blood-stream (see Supplementary Video2). Scale bar, 100  $\mu$ m. (I) The circulating neutrophils in the mesentery vessel were counted in each group. \*\*\*P < 0.001 vs. PBS. (J) Whole blood of CLP mice was withdrawn 24 h after CLP and applied to a MC-FAN. The red arrowheads indicate the leukocytes attached to the tops of microcapillaries. (K) The time required for the passage of 100  $\mu$ l of whole blood was determined using a MC-FAN in four groups. \*P < 0.05 and †P < 0.05 vs. PBS and HSA, respectively. The results shown are the means  $\pm$  SEM of five mice (A, C, E, F, I and K) or ten healthy volunteers and five septic patients (G). Ten mice were used in each group (B and D).

Figure 2. Effects of HRG treatment on inflammation in lungs and kidneys of CLP mice.

(A) CLP mice treated with PBS, HSA, or HRG were fixed at 24 h after CLP.

Paraffin-embedded sections of the lungs (upper) and kidneys (lower) were stained with HE. (B) Edema of the lung was evaluated in each group as a ratio of wet to dry lung tissue weight. \* $P < 0.05$ , ††† $P < 0.001$  vs. PBS and HSA, respectively. (C) The lungs of CLP mice were stained by DAPI (nuclei: blue), anti-Gr-1 antibody (neutrophil: green), anti-CD42d antibody (platelet: orange), and anti-fibrinogen/fibrin antibody (fibrin: red) followed by fluorescence detection. Red arrowheads indicate Gr-1, CD42d, and fibrin triple positive sites. (D) Neutrophils in the lungs were counted in each group. \*\*\* $P < 0.001$ , ††† $P < 0.001$  vs. PBS and HSA, respectively. (E) The relative percentages of CD42d and fibrin/fibrinogen sites among Gr-1 positive neutrophils were determined. \*\*\* $P < 0.001$  vs. sham. (F) The number of Gr-1, CD42d, and fibrin triple positive sites in the lungs was counted in each group. \*\*\* $P < 0.001$ , ††† $P < 0.001$  vs. PBS and HSA, respectively. (G) The lungs of CLP mice were stained by SYTOX Blue (nuclei: blue) and anti-Gr-1 antibody (neutrophil: red) followed by fluorescence detection. Yellow arrowheads indicate NET. (H) NETs in the lungs were counted in each group. \*\*\* $P < 0.001$ , ††† $P < 0.001$  vs. PBS and HSA, respectively. (I) Determination of mRNAs of TNF- $\alpha$ , IL-6, PAI-1, iNOS, neutrophil elastase, and RAGE in lungs of CLP mice. The tissue samples for real-time PCR were collected 24 h after CLP. The relative expression levels were calculated treating sham control as one unit.

**\*\*P**< 0.01 vs. PBS. **†P**< 0.05 and **††P**< 0.01 vs. HSA. The results shown are the means  $\pm$  SEM of five mice (**B**, **D**, **E**, **F**, **H** and **I**). Scale bars, 50  $\mu$ m (**A** and **C**). Scale bars, 20  $\mu$ m (**G**).

Figure 3. Effects of HRG treatment on the number of blood cells, coagulation, and hypercytokinemia in CLP mice.

(**A**) The whole blood samples were collected 24 h after CLP. The results shown are the means  $\pm$  SEM of five mice. **\*\*P**< 0.01 vs. PBS. **†P**< 0.05 and **††P**< 0.01 vs. HSA.

(**B**) The plasma samples for coagulation test were collected 24 h after CLP. The results shown are the means  $\pm$  SEM of six mice. **\*\*P**< 0.01, **\*\*\*P**<0.001 vs. PBS. **†P**< 0.05 and **†††P**< 0.001 vs. HSA. (**C**) The serum samples for the determination of cytokines

were collected 24 h after CLP. The results shown are the means  $\pm$  SEM of five mice.

**\*P**< 0.05, **\*\*P**<0.01 vs. PBS. **†P**< 0.05 and **††P**< 0.01 vs. HSA.

Figure 4. HRG's spherical-shape-inducing and adhesion-increasing effects on purified human neutrophils.

(**A**, **H** and **I**) Purified human neutrophils were labeled with calcein-AM (green) and Hoechst33342 (blue) for 20 min. The neutrophils were incubated with reagents (1

$\mu\text{M}$ ) on polystyrene surface (**A**) or a monolayer of EA.hy926 (**H** and **I**) for 60 min and the neutrophil shape was observed under a fluorescent microscope (**A** and **I**) or a differential interference contrast microscope (**H**). (**B** and **J**) The rounding of neutrophils was analyzed by the In Cell Analyzer. Form factor (max diameter/ min diameter) was determined. One unit represents an ideal spherical shape. \* $P < 0.05$ , \*\*\* $P < 0.001$  vs. HBSS. † $P < 0.05$ , ††† $P < 0.001$  vs. BSA. ‡‡ $P < 0.01$ , ‡‡‡ $P < 0.001$  vs. HSA. §§§ $P < 0.001$  vs. fMLP. (**C** and **K**) After gentle washing of the microtiter plate with HBSS twice, the residual cell numbers were counted and expressed as percentages of the initial cell numbers. \*\*  $P < 0.01$ , †† $P < 0.01$ , ‡‡ $P < 0.01$ , and §§ $P < 0.01$  vs. HBSS, BSA, HSA, and fMLP, respectively. (**D**) The concentration-effect curve was drawn by the plot of a spherical shape at different concentrations of HRG. The maximal roundness at 1  $\mu\text{M}$  of HRG was expressed as 100%. (**E**) Effects of polyclonal antibody against HRG on HRG-induced induction of spherical shape in neutrophils. Anti-HRG Ab (300  $\mu\text{g/ml}$ ) or control IgG was added simultaneously with HRG and the incubation continued for 60 min. (**F**) Quantitative analysis of the effects of specific antibodies against HRG on neutrophil shape. \*\*\* $P < 0.001$  and ††† $P < 0.001$  vs. HBSS and HRG+IgG groups, respectively. (**G**) Effects of specific antibody against HRG on adhesion of neutrophils. \*\*\* $P < 0.001$  and † $P < 0.05$  vs. HBSS and HRG+IgG,

respectively. The results shown are the means  $\pm$  SEM of three experiments (**B**, **C**, **D**, **F**, **G**, **J** and **K**). Scale bars, 20  $\mu$ m (**A**, **D**, **E**, **H** and **I**).

Figure 5. Relationship between neutrophil surface structure and passage through microcapillaries and effects of uptake of HRG by neutrophils.

(**A** and **B**) The purified human neutrophils were incubated with reagents at 1  $\mu$ M on a cover glass for 60 min at 37°C. Scanning electron microscopic pictures of neutrophils were obtained. Time-dependent changes in the shapes (**B**). (**C**) The purified human neutrophils were incubated as in (**A**). The neutrophils were stained with Alexa Fluor 594-labelled phalloidin (red) for F-actin and Alexa Fluor 488-labelled DNase I (green) for G-actin. Cell nuclei were stained with DAPI (blue). Scale bars, 5  $\mu$ m (**A** and **C**), 10  $\mu$ m (**B**). (**D**) The purified human neutrophils were incubated with reagents at 1  $\mu$ M for 60 min and then applied to a MC-FAN. Red arrowheads indicate the leukocytes attached to the upper chamber. White arrowheads indicate the leukocytes attached to the microcapillary entrance. (**E** and **G**) The time required for the passage of 100  $\mu$ l neutrophil suspension through the MC-FAN was determined. \* $P < 0.05$ ,  $\dagger\dagger P < 0.01$ ,  $\ddagger P < 0.05$ , and  $\S\S\S P < 0.001$  vs. HBSS, BSA, HSA, and fMLP, respectively (**E**). \* $P < 0.05$  vs. IgG control (**G**). (**F**) The anti-coagulated whole blood treated with anti-HRG

Ab or control IgG was applied to the MC-FAN. White arrowhead indicates the leukocyte attached on the microcapillary entrance. The results shown are the means  $\pm$  SEM of five experiments (**E** and **G**).

Figure 6. Analysis of signal transduction pathways for HRG's effects on neutrophils.

(**A**) The neutrophils were loaded with BAPTA-AM (50  $\mu$ M) or DMSO for 20 min and incubated with HRG (1  $\mu$ M) for 60 min. (**B**) The neutrophils were loaded with Fluo-4-AM for 20 min and incubated with reagents at 1  $\mu$ M for 60 min. Intracellular calcium was monitored by Fluo-4 fluorescence. (**C**) The average of fluo-4 fluorescence intensity was calculated by In Cell Analyzer. \*\*\* $P$  < 0.001, ††† $P$  < 0.001, ‡‡‡ $P$  < 0.001, and §§§ $P$  < 0.001 vs. HBSS, BSA, HSA, and fMLP, respectively. (**D**) The neutrophils were preincubated with Toxin B (100 ng/ml) or PBS for 90 min and then incubated with HRG (1  $\mu$ M) for 60 min. (**E**) The neutrophils were incubated with reagents at 1  $\mu$ M for 15 min, and the ROS produced extracellularly was determined using iso-luminol as a substrate. The chemiluminescence in the medium was determined by a plate reader. \*\*\* $P$  < 0.001, ††† $P$  < 0.001, and ‡‡‡ $P$  < 0.001 vs. HBSS, BSA, and HSA, respectively. (**F**) The neutrophils were loaded with CM-H<sub>2</sub>DCFDA for 20 min and incubated with reagents at 1  $\mu$ M for 60 min. The fluorescence of DCF



was detected by the In Cell Analyzer. \*\*\* $P < 0.001$ , †† $P < 0.01$ , and ‡‡‡ $P < 0.001$  vs. HBSS, BSA, and HSA, respectively. **(G-K)** Monolayer of EA. hy926 cells were stimulated with LPS (10ng/ml) or TNF- $\alpha$  (10ng/ml) in the presence of HBSS, HSA or HRG for 30 min at 37 °C. The cells were stained by anti-human ICAM-1 Ab (**G** and **H**), anti-human P-selectin Ab (**I** and **J**) or anti-phosphatidylserine Ab (**K** and **L**), for 25 min at 4 °C. **(G-J)** (-) is no stimulated-sample. **(H, J and L)** ICAM-1 (**H**), P-selectin (**I**) or Phosphatidylserine (**J**) -positive cells were counted in each group. \* $P < 0.05$ , \*\*\* $P < 0.001$  vs. LPS+HBSS. † $P < 0.05$ , ††† $P < 0.001$  vs. LPS+HSA. ‡ $P < 0.05$ , ‡‡ $P < 0.01$ , ‡‡‡ $P < 0.001$  vs. TNF- $\alpha$ +HBSS. § $P < 0.05$ , §§ $P < 0.01$ , §§§ $P < 0.001$  vs. TNF- $\alpha$ +HSA. The results shown are the means  $\pm$  SEM of three experiments (**C**, **E** and **F**), four fields (**H** and **J**) or six fields (**L**). Scale bars, 20  $\mu$ m (**A**, **B** and **D**), 50  $\mu$ m (**G**, **I** and **K**).

## Supplementary figure legends

### Supplementary Figure 1

Effects of HRG on CLP mice. (A) Sickness behaviors were evaluated at 24 h after CLP using a 4-point rating scale. The results shown are the means  $\pm$  SEM of 18 mice from each group. \*\*\* $P < 0.001$ , ††† $P < 0.001$  vs. PBS and HSA, respectively. (B) Kaplan-Meier survival curve of mice with CLP. PBS, HSA (20 mg/kg), or human purified HRG (20 mg/kg) was administered i.v. 6, 24, and 48 h after CLP. (C) Bacterial number in CLP mouse blood. Bacterial numbers in the blood were evaluated by counting the colony-forming units of whole blood from each group. The results shown are the means  $\pm$  SEM of five mice. (D) Infiltrating cell number in the peritoneal cavity. The recovered washing fluid of the peritoneal cavity was used to count the infiltrating cells in each group. The results shown are the means  $\pm$  SEM of five mice. (E) The hematocrit of whole blood in CLP mice. The hematocrit of mice was determined 24 h after CLP in four groups. The results shown are the means  $\pm$  SEM of five mice.

### Supplementary Figure 2

Immunohistochemical localization of HRG in the lung of septic mice. (A) The lungs

of CLP mice were stained by DAPI (nuclei: blue), anti-Gr-1 antibody (neutrophil: green), anti-HRG antibody (orange), and anti-fibrinogen/fibrin antibody (fibrin: red) followed by fluorescence detection. Yellow arrowheads indicate HRG-positive clot. Scale bar, 50  $\mu$ m. (B) Higher magnification of typical fibrin-negative neutrophils with HRG-immunoreactivity in sham mice. Red arrowheads indicate HRG-positive sites. Scale bar, 5  $\mu$ m

### Supplementary Figure 3

HRG's spherical-shape-inducing effects on purified human neutrophils. (A) Time-dependence of the spherical shape-inducing effects of HRG on neutrophils. The neutrophils were incubated with 1  $\mu$ M of HRG for 5, 10, 15, 30, and 60 min after the addition of HRG, respectively. (B) The reversibility of a neutrophil's shape from flattened to spherical by the addition of HRG. The neutrophils were incubated in HBSS for 60 min and then HRG (1  $\mu$ M) was added to the medium. Morphological changes were observed at 60 and 120 min after the addition of HRG. Scale bars, 20 $\mu$ m (A and B).

### Supplementary Figure 4

Effects of HRG on human PBMCs adhesion on vascular endothelial cells. (A) Purified human PBMCs were labeled with calcein-AM (green) and Hoechst33342 (blue) for 20 min. The PBMCs were incubated with reagents (1  $\mu$ M) on a monolayer of EA.hy926 for 60 min and the shapes of PBMCs were observed under a fluorescent microscope. After gentle washing of the microtiter plate with HBSS twice, the residual cells were observed under a fluorescent microscope. (B) The residual cells were counted and expressed as % of the initial cell numbers. Scale bars, 20  $\mu$ m.

#### Supplementary Figure 5

Chemotactic effects of HRG on human neutrophils. (A) HRG's effects on vertical transfer of neutrophils through micropores. Purified neutrophils ( $5 \times 10^5$  cells) were added to the upper part of a Boyden chamber. The transfer of neutrophils into a lower chamber containing HRG (0.03-1  $\mu$ M), BSA (1  $\mu$ M), HSA (1  $\mu$ M), and fMLP (1  $\mu$ M) was measured at 37 °C 60 min later. The results shown are the means  $\pm$  SEM of three experiments. \*  $P < 0.05$  and \*\*  $P < 0.01$  vs. HBSS. (B) HRG's effects on the horizontal migration of neutrophils in agarose gel. The purified neutrophils ( $5 \times 10^5$  cells) were added to one well in agarose gel (5 mm thick) and were allowed to migrate toward the other well (2 mm apart) containing a possible chemoattractant (1  $\mu$ M). The

results shown are the means  $\pm$  SEM of three experiments. \*\*  $P < 0.01$  vs. HBSS.

#### Supplementary Figure 6

The uptake of HRG by neutrophils. (A) Uptake of fluorescein-labelled HRG by neutrophils. The Hoechst33342-stained neutrophils were incubated with fluorescein-HRG or fluorescein-HSA for 60 min. (B) Higher magnification of typical neutrophils with fluorescein-HRG inside. (C) The average number of fluorescent granules was counted. \*\*\* $P < 0.001$  and  $\dagger\dagger\dagger P < 0.001$  vs. HBSS.  $\ddagger\ddagger\ddagger P < 0.001$  vs. HSA. The results shown are the means  $\pm$  SEM of five experiments. Scale bars, 20  $\mu\text{m}$  (A), 10  $\mu\text{m}$  (B). (D) Binding of fluorescein-labelled HRG on EA.hy926. The Hoechst33342-stained EA.hy926 cells were incubated with fluorescein-HRG or fluorescein-HSA for 60 min, and the cells were photographed under fluorescent microscopy after washing. Differential interference contrast microscopic observation was performed. (E) The even distribution of fluorescein-HRG binding was observed on EA.hy926. Scale bars, 20  $\mu\text{m}$  (D and E).

#### Supplementary Figure 7

Effects of different kinds of protein kinase inhibitors on HRG effects on neutrophils.

(A, B and C) After loading calcein and Hoechst33342, PI-3 kinase inhibitors; LY294002 (5 and 50  $\mu$ M) or wortmannin (10 and 100 nM) (A), MAP kinase inhibitors; SB239063 for p38, FR180204 for ERK, or SP600125 for JNK (1 and 10  $\mu$ M each) (B) or Syk inhibitor; BAY61-3606 (10 and 100  $\mu$ M) (C) was added to the incubation medium. The neutrophil shape was observed 60 min thereafter. \* $P$ < 0.05, \*\* $P$ < 0.01, and \*\*\* $P$ < 0.001 vs. HBSS. Scale bars, 20 $\mu$ m

#### Supplementary Figure 8

FACS analysis of human neutrophils. C5a, IL-8 or fMLP were preincubated with HSA or HRG for 60 min at 37 °C. Purified human neutrophils were stimulated with the mixture for 60 min at 37 °C in 5% CO<sub>2</sub> atmosphere. The neutrophils were stained by FITC-labeled anti-human CD11b Ab, FITC-labeled anti-human activated CD11b Ab, FITC-labeled anti-human CD62L Ab or PE-labeled anti-human CD162 Ab for 25 min at 4 °C. The fluorescence intensity of the cells was analyzed on a FACS calibur.

#### Supplementary Figure 9

Effects of increasing concentrations of IL-8 and C5a on the shapes of HRG-induced neutrophils. The neutrophils were incubated with increasing concentrations of IL-8 or

C5a (1- 100 ng/ml) in the presence of HRG (1  $\mu$ M). Scale bar, 20  $\mu$ m.

#### Supplementary Figure 10

Scheme of the effects of HRG on septic condition. A plasma protein HRG decreased markedly in septic mice with high lethality. Supplementary treatment with HRG improved the survival of septic mice by inhibiting immunothrombosis, DIC and excessive tissue inflammation. HRG kept circulating neutrophils quiescent morphologically and functionally.

## **Supplementary video legends**

### **Supplementary Video 1**

Behavioral changes in sepsis mice treated with HRG. Sepsis was induced by CLP and the mice were treated with PBS, HSA (20 mg/kg, i.v.), or HRG (20 mg/kg, i.v.). The locomotor activity of the mice in each group was monitored by a video camera 24 h after the induction of sepsis.

### **Supplementary Video 2**

*In vivo* imaging of circulating neutrophils in the venules in CLP sepsis mice. FITC-labelled anti-Gr-1 antibody (1 mg/kg) was injected i.v. to CLP mice treated with PBS or HRG (20 mg/kg, i.v.). The immunostained neutrophils in the mesenteric venules were observed by a high-speed scan spinning-disk confocal microscopy system.

### **Supplementary Video 3**

HRG's effects on the passage of blood through microchannels. Whole blood of CLP mice treated with PBS, HSA (20 mg/kg, i.v.), or HRG (20 mg/kg, i.v.) was withdrawn from the abdominal aorta 24 h after CLP and applied to a MC-FAN. The passage of blood cells was monitored by a CCD camera.



#### Supplementary Video 4

HRG's effects on the passage of neutrophils in microcapillaries. The purified human neutrophils were incubated with BSA, HSA, HRG, or fMLP at 1  $\mu$ M for 60 min at 37 °C and applied to a MC-FAN. The passage of neutrophils through microcapillaries was monitored by microscope-CCD camera system in the apparatus.

#### Supplementary Video 5

Effects of anti-HRG Ab on the passage of human whole blood in microcapillaries. The human whole blood was treated with anti-HRG Ab (40  $\mu$ g/ml) or control IgG for 30 min at 37 °C and applied to MC-FAN. The passage of blood cells through the microcapillaries was monitored as described above.

Figure 1

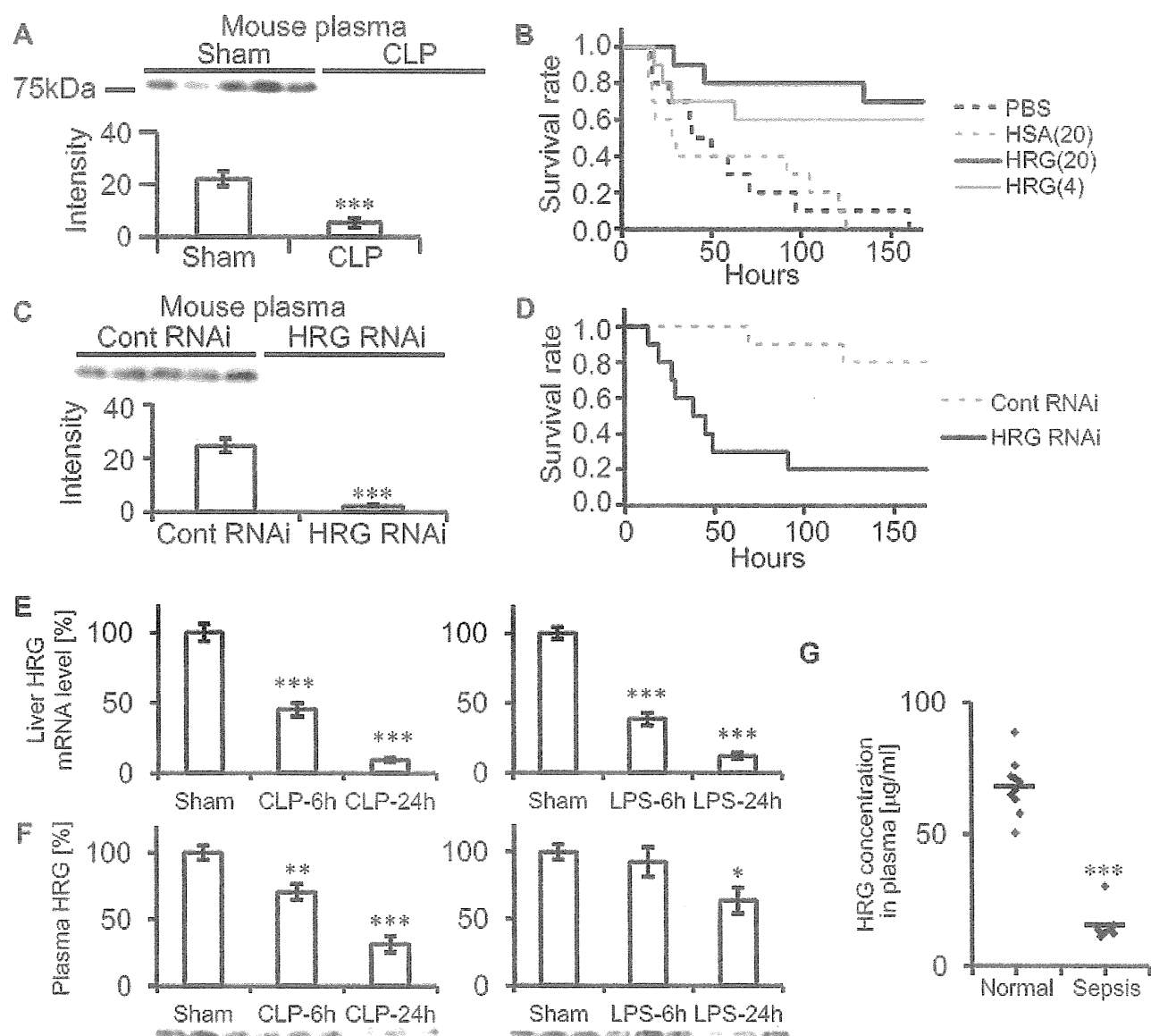


Figure 1

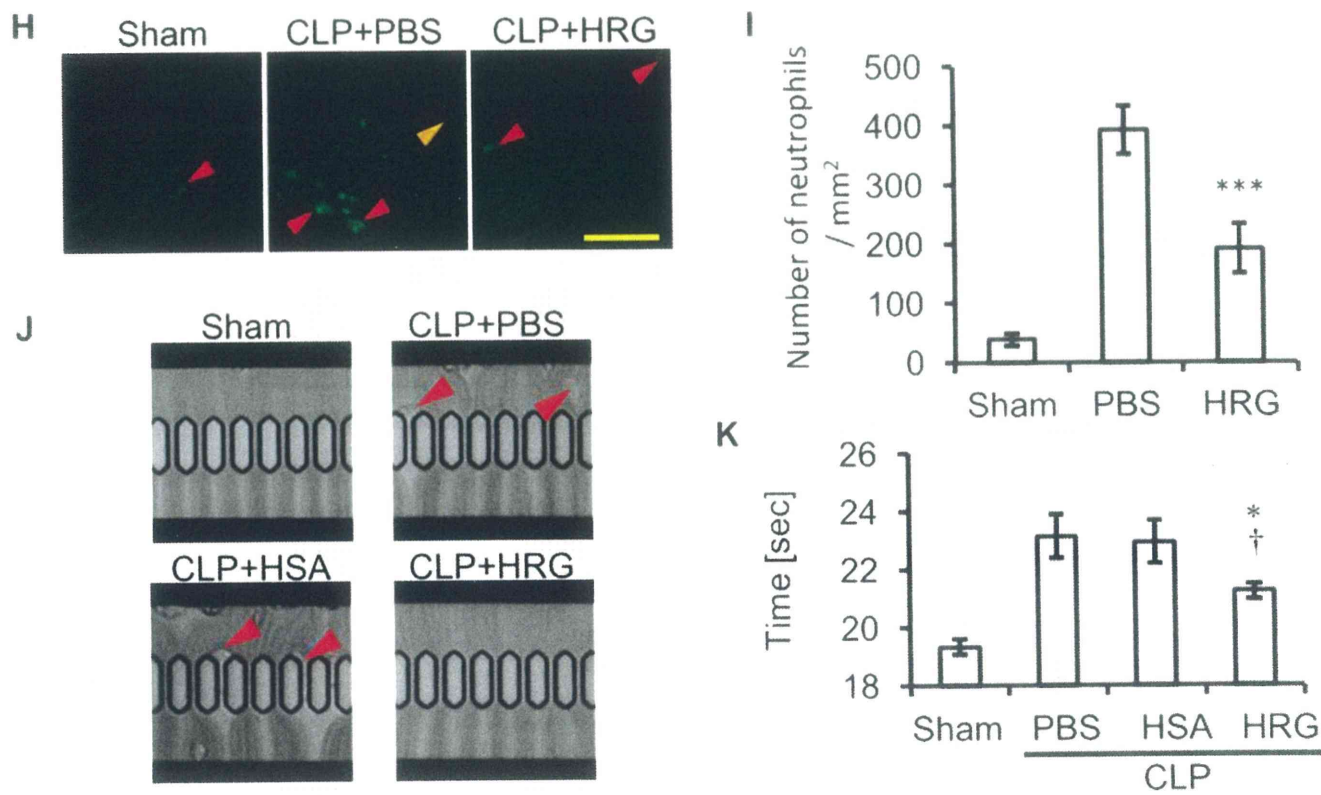


Figure 2

